Interactions between alkali metals and oxygen on a reconstructed surface: An STM study of oxygen adsorption on the alkali-metal-covered Cu(110) surface

R. Schuster, J. V. Barth, J. Wintterlin, R. J. Behm,* and G. Ertl
Fritz-Haber-Institut der Max-Planck-Gesellschaft, Faradayweg 4-6, D-14195 Berlin, Germany
(Received 8 August 1994)

Room-temperature adsorption of oxygen on potassium- and cesium-precovered Cu(110) surfaces was studied by scanning tunneling microscopy. Depending on the alkali-metal precoverage, two different scenarios exist for the structural evolution of the surfaces. For alkali-metal coverages $\theta_{alk} \leq 0.13$ ML [$\theta_{alk}=0.13$ corresponds to the (1×3) missing-row reconstructed Cu(110) surface], oxygen adsorption leads first to a transient contraction of the missing rows into islands of a (1×2) structure. After longer exposures it causes the local removal of the alkali-metal-induced reconstruction, and the (2×1) Cu-O "added-row" structure with $\theta_O=0.5$ is formed. In this structure the alkali-metal atoms are incorporated in the Cu-O chains. For higher alkali-metal precoverages, in the range of the (1×2) reconstruction ($\theta_{alk}\approx0.2$), more than one-half a monolayer of oxygen can be incorporated into the (1×2) phase with only a minor structural effect before, at higher oxygen coverages, complex oxygen–alkali-metal–Cu structures with oxygen coverages well above 0.5 ML are formed. The saturation oxygen coverage is drastically enhanced beyond $\theta_O=0.5$, the quasisaturation value of the clean surface. Based on mass-transport arguments the substrate is reconstructed for all ratios of oxygen and alkali metal investigated here. Hence, adsorbate-substrate interactions are essential for these structures; they are not dominated by interactions between alkali metals and oxygen, i.e., by adsorbate-adsorbate interactions.

I. INTRODUCTION

Coadsorption of different adsorbates often leads to significant modifications of the chemical and structural properties of the respective adsorbates by the formation of mixed adlayers or even by surface compound formation. The interaction between alkali metals and oxygen, coadsorbed on metal surfaces, is of particular interest because of its relevance for various catalytic processes. It is known that on catalysts for ammonia synthesis the alkali metal is present on the surface not as a bulk oxide but as a chemically different species which is bound to the Fe surface, together with oxygen.[1] This raises questions on the chemical nature of the interactions between the adsorbed alkali metals and oxygen atoms. Both direct bonds or substrate mediated interactions appear plausible. Here we present a scanning tunneling microscopy (STM) study on the structural and mechanistic aspects of the coadsorption of alkali metals and oxygen on a Cu(110) surface. By exploiting the fact that both of these adsorbates interact strongly with the substrate and lead to characteristic reconstructions of the substrate already at room temperature, we gain information on the coadsorption behavior and on the role of substrate-adsorbate interactions in the resulting surface phases. The first evidence, to our knowledge, of a change in the surface reconstruction during oxygen adsorption on an alkali-metal precovered fcc(110) surface was found in a low-energy electron diffraction (LEED) study on O/K/Ni(110) (Ref. 2) where at sufficiently low alkali-metal precoverages a transient (1×2) phase is formed which finally transforms into a (2×1) phase. At higher alkali-metal precoverages, complex superstructures were observed.

The (reconstructive) adsorption behavior of the binary systems, O/Cu(110) and alkali-metal/Cu(110), has been studied extensively in the recent past, in particular by STM. Alkali-metal adsorption on Cu(110) at room temperature results in a series of missing-row reconstructions where the alkali atoms form a dilute phase, embedded in the troughs of the missing rows. At low coverages, the reconstruction is a local process where individual alkali-metal atoms replace two or three Cu atoms from the close-packed $[1\bar{1}0]$ Cu rows and are adsorbed in the resulting holes. With increasing coverage, these nuclei arrange into ordered (1×3) ($\theta_{alk}=0.13$) and (1×2) phases ($\theta_{alk}\geq0.2$).[3–7] [The coverage θ refers to the Cu atom density in the topmost unreconstructed Cu(110) surface.] Similar structures with only small structural differences between the various alkali metals have been reported for alkali-metal adsorption on a number of fcc(110) surfaces such as Ni(110), Ag(110), and Pd(110) which signals a universal behavior of these unreconstructed surfaces upon alkali-metal adsorption (see Ref. 8 and references therein).

Oxygen adsorption on the Cu(110) surface at room temperature leads to an almost instantaneous (2×1) reconstruction, via island formation, where chains of alternating oxygen and Cu atoms run along the [001] direction.[9–11] This is perpendicular to the direction of the atomic rows in the alkali-metal-induced missing-row reconstruction. The oxygen coverage in this phase is $\theta_O=0.5$. Only at very high oxygen doses, at about 16.000 L (1 L$=10^{-6}$ Torr s) at room temperature, a

 ©1994 The American Physical Society

$c(6\times2)$ phase with $\theta_O=\frac{2}{3}$ is formed.[12,13]

Based on the reactivity of alkali metals with oxygen one might expect that the coadsorption of oxygen and alkali metals is dominated by attractive interactions or even compound formation of the two adsorbates. We show here that for alkali-metal coverages up to $\theta_{alk}=0.2$, substrate-adsorbate interactions continue to play an important role and that the observations can be fully rationalized only when the various reconstructions of the substrate are also taken into consideration. (Based on reports of Clendening *et al.*, a coverage of $\theta_{alk}=0.48$ corresponds to 1 ML of cesium on Cu(110);[14] $\theta_{alk}=0.2$, therefore, is approximately one-half a physical monolayer.) The resulting structures are determined by the competition between three bonds: that between the alkali metal and the oxygen and those of the two adsorbates with the substrate. It will be shown that it depends on the respective coverages which of these interactions is the most dominant.

In the experiments presented here we investigated structural changes that occur upon oxygen adsorption on a submonolayer alkali-metal precovered Cu(110) surface by STM. Two different alkali-metal precoverages were used: In the first part of the paper, we will present data obtained for an alkali-metal precoverage of $\theta_{alk}\leq0.13$, where the Cu(110) surface is (1×3) reconstructed. The second part of the paper deals with alkali-metal precoverages around $\theta_{alk}=0.2$, which induce a (1×2) reconstruction of the Cu(110) surface. In this case, complex structures are formed upon subsequent oxygen adsorption, which differ considerably from those at lower alkali-metal coverages and also from those formed by the individual adsorbates. The structural and mechanistic implications of these results and their relation to existing data are finally presented in the conclusions.

II. EXPERIMENT

The experiments were performed in a UHV system (base pressure: 1×10^{-10} Torr) equipped with a "pocket size" STM and facilities for LEED, Auger electron spectroscopy (AES) using a cylindrical mirror analyzer, and ion sputtering. The Cu(110) surface was cleaned by repeated sputter and annealing cycles until no impurities could be detected by AES and a sharp (1×1) pattern had evolved in LEED. The alkali metal was evaporated from commercially available SAES getter sources. The coverages were determined by AES, from the *LMM* transition at 252 eV for K, from the *MNN* peak at 563 eV for Cs, and from the *KLL* Auger peak at 510 eV for oxygen. The absolute potassium coverage was calibrated by use of the $c(2\times2)$ structure formed at $\theta_K=0.50$ on the Au(110) surface.[15] The Cs coverage was calibrated by assuming a coverage of $\theta_{Cs}=0.13$ for the (1×3) structure on Cu(110).[3] For calibration of the O coverage the (2×1) reconstruction formed at $\theta_O=0.5$ on Cu(110) was used.[9,10] The STM images are colored with a gray scale according to height. Brighter areas correspond to higher levels. The tunneling conditions are given in the figure captions. The tunneling voltage is the potential of the sample with respect to the tip. Further experimental details are given in Ref. 6.

III. RESULTS AND DISCUSSION

A. Oxygen adsorption for $\theta_{alk}\leq0.13$

First, we present oxygen uptake curves on the alkali-metal precovered surface determined by AES. A set of data measured for the O/Cs/Cu(110) system is shown in Fig. 1. They indicate an enhancement of the initial O-sticking coefficient by more than a factor of 2 for $\theta_{Cs}=0.11$, compared with that of the clean Cu(110) surface. For Cs coverages below $\theta_{Cs}=0.15$, the oxygen adlayer reaches an apparent saturation coverage of $\theta=0.5$ at approximately 10 L. For doses in excess of 10 L, oxygen uptake proceeds much slower. Similar results are obtained for K/Cu(110). For the pure O/Cu(110) system further oxygen uptake above $\theta_O=0.5$ leads to a $c(6\times2)$ phase with $\theta_O=\frac{2}{3}$ which was saturated at ~16.000 L. We note in advance that the same structure develops on the alkali-metal precovered surface, but the oxygen exposures required are significantly lower: The $c(6\times2)$ structure begins to form already after additional 850 L of oxygen. Hence the increase in the oxygen sticking coefficient caused by preadsorbed alkali metal is also found in the higher oxygen coverage regime. In total, the kinetics of the O/Cu(110) interaction are strongly affected by the coadsorbed alkali metals already in the low alkali-metal coverage regime. The data for alkali-metal coverages $\theta_{alk}>0.15$ in Fig. 1 will be discussed in the next section.

The structural effects of oxygen adsorption on alkali-precovered Cu(110) are illustrated in a set of selected STM images from a series recorded during oxygen adsorption on the K-precovered, (1×3) reconstructed Cu(110) surface ($\theta_K=0.13$) (Fig. 2). The oxygen doses are indicated in the figures. Up to 24 L [Fig. 2(f)], the oxygen pressure was about 7×10^{-9} Torr. For the final exposure of 850 L shown in Fig. 2(g) the oxygen pressure was raised to 1×10^{-6} Torr. The time intervals between the STM images were of the order of a few minutes. During the experiment the scanned area drifted by about $\frac{2}{3}$ of the width of the image towards the left side. From comparison of STM measurements of O-adsorption on

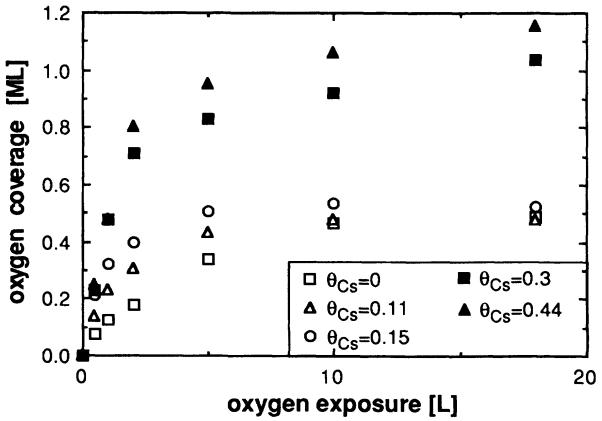

FIG. 1. Oxygen uptake curves on Cs/Cu(110) at 300 K. The Cs coverages are as indicated. The oxygen pressure was 1×10^{-9} Torr.

the clean Cu(110) surface with the results of the O-uptake curves in Fig. 1, the effective doses in the STM images are determined to be about two times lower than in Fig. 1, due to shadowing effects of the tip.

Figure 2(a) shows a part of a large (1×3) reconstructed terrace. The dark stripes correspond to the K-filled troughs of the reconstruction, which in this case are imaged as indentations. The K atoms are invisible in these images, as it is mostly the case with the K/Cu(110) system.[16] After an oxygen exposure of 0.5 L the previously almost perfect (1×3) reconstruction is locally destroyed

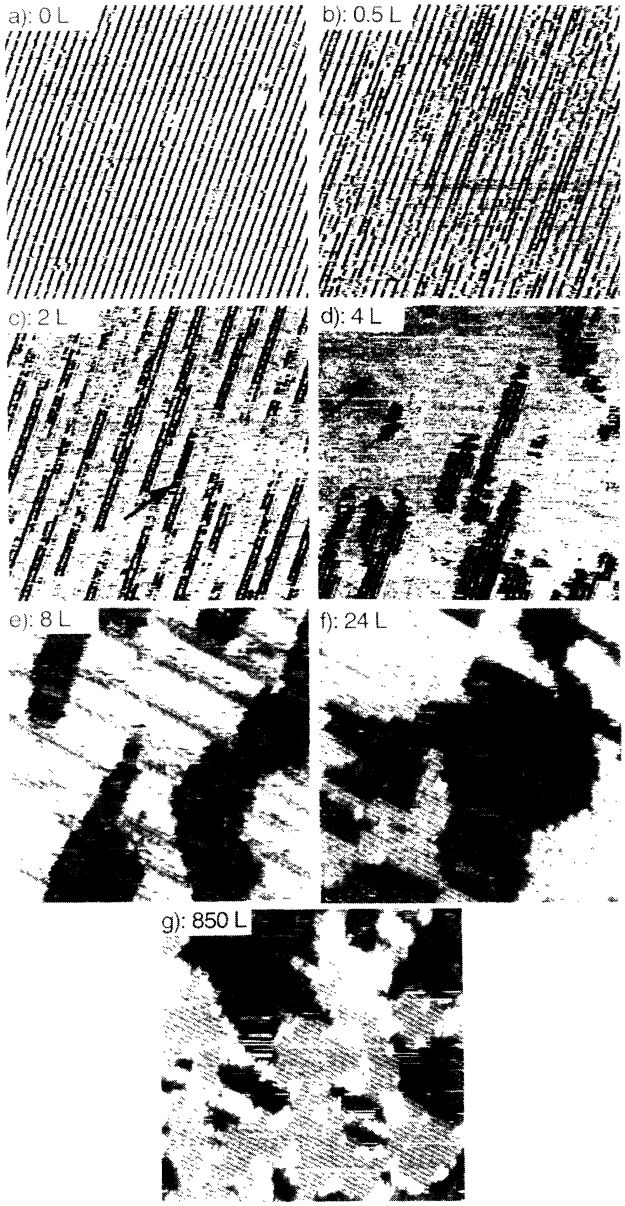

FIG. 2. STM images recorded during oxygen adsorption on the potassium-precovered Cu(110) surface, with $\theta_K=0.13$ (360×360 Å^2; $U_T=-0.03$ V, $I_T=6.3$ nA). The oxygen doses are indicated. In Fig. 2(c) the dissolution of [1$\bar{1}$0]Cu rows in the (1×2) structure and in Fig. 2(d) the nucleation of the (2×1)O structure are marked with arrows.

[Fig. 2(b)]. Several missing-row troughs have moved together to form local (1×2) units, which mostly extend over only two missing-row troughs in the [001] direction. After a total exposure of 2 L [Fig. 2(c)] the (1×3) missing-row structure has been completely removed and the surface topography is dominated now by individual (1×2) missing-row entities. Their average length along [1$\bar{1}$0] is now about 100 Å, while before oxygen adsorption the missing-row troughs extended over the entire terraces. Simultaneously also the total area covered by the missing-row troughs is reduced by about 30% as compared to the initial surface. If we assume the Cu surface atoms to be in a (1×1) configuration in the flat parts of the surface, the decrease in the missing-row reconstructed area corresponds to an increase in the density of topmost layer Cu atoms by about 0.1 ML, which requires substantial mass transport of Cu atoms. Additionally, in some of the (1×2) elements even the central Cu-[1$\bar{1}$0] row has been removed [see the arrow in Fig. 2(c)].

Both the removal and the clustering of missing-row troughs in (1×2) structures continue to higher oxygen exposures. After an oxygen dose of 4 L in total the missing-row troughs have decreased by another 50% and the (1×2) islands now consist of up to ten (1×2) rows. At the same time, the first indications of a new structure are seen as faint gray lines along the [001] direction [one is marked by an arrow in Fig. 2(d)]. After an exposure of 5–6 L these lines have stabilized and form small troughs along [001], orthogonal to the (1×2) row direction. They closely resemble individual Cu-oxygen chains of the "added-row" phase, observed for the pure binary system O/Cu(110).[9–11,17] The formation of these (2×1) nuclei on the potassium-precovered surface, however, starts at much higher oxygen coverages as compared to the clean Cu(110) surface: Considering the data in Fig. 1 (corrected for the shadowing of the tip) the oxygen coverage is about $\theta_O=0.2$ for an exposure of 4 L. In contrast, on the clean Cu(110) surface, nuclei of the (2×1) structure form instantaneously at room temperature at the lowest investigated coverage, and for $\theta_O=0.2$ 40% of the surface is covered with the (2×1) added-row phase. The most plausible reason is that the adsorbed oxygen is removed from the system by reaction with the adsorbed alkali atoms up to a critical coverage. Only after this coverage is exceeded can the (2×1)O phase start to form. Additionally, the consumption of Cu atoms for the filling of the missing-row troughs and the formation of the Cu-O chains are competitive processes. Hence the formation of the (2×1) nuclei might be retarded by a lack of Cu atoms.

After an oxygen exposure of 8 L the (2×1) nuclei have grown to small stripes of the (2×1) added-row reconstruction [Fig. 2(e)], which are resolved as gray stripes normal to the former alkali-metal-induced rows [note that due to electronic effects and tip condition the (2×1) added rows are imaged as indentations in this image[9]]. The (1×2) structure of the alkali-metal reconstruction has completely disappeared. In addition, monolayer deep holes have formed, preferentially on the previously (1×2) reconstructed area [cf. Figs. 2(d) and 2(e)]. Apparently, the edges of the (1×2) areas can supply Cu

atoms for the buildup of the (2×1) added-row structure on the unreconstructed surface areas more efficiently than the clean parts of the surface. For the clean Cu(110) surface, steps are the main source of Cu atoms during its reaction with oxygen.[9,10,17]

Growth of the (2×1) phase proceeds with further oxygen exposure and after a 24-L exposure, practically the whole surface is (2×1) reconstructed [Fig. 2(f)]. LEED images of such a surface show clear, sharp (2×1) spots, indistinguishable from those seen for the pure O/Cu(110) system. At this point, the oxygen coverage as determined by AES has reached a value close to $\theta_O=0.5$. Hence, at the first glance, the potassium preadsorption does not influence the structure of the (2×1) O/Cu(110) reconstruction. Closer inspection, however, reveals that the (2×1) added rows display many defects, which were not observed in the binary O/Cu(110) system and which are associated with the alkali atoms, as discussed later (see Fig. 3).

During the next 100 L only minor changes of the surface structure are observed. The (2×1) reconstruction is completed during this stage. In addition, some white protrusions are formed, mainly near step edges. Their number increases with higher oxygen exposures, and after an oxygen dose of 850 L [Fig. 2(g)], they start forming islands with a regular structure. This structure and the protrusions very much resemble the features of the $c(6\times2)$ O/Cu(110) structure in the pure O/Cu(110) system,[12,13] and in analogy the white protrusions are interpreted as nuclei of the $c(6\times2)$ structure. The minimum dose required for the beginning of the formation of the $c(6\times2)$ structure, however, is about one order of magnitude lower on the K-precovered surface than on the clean Cu(110) surface at room temperature.

The question of the locations of the K adatoms in the (2×1)O structure can be answered more clearly from a similar STM experiment, where the tip and imaging conditions were different from before: The Cu-O added rows appear as protrusions. The potassium precoverage is again $\theta_K=0.13$. The sequence of surface structures is the same as in the previous experiment. In this imaging mode the added rows of the growing (2×1) phase show many defects which appear as interruptions of the rows (Fig. 3). The apparent width of the defects is about 3–4 Å, which corresponds to one substrate lattice constant along [001]. The asymmetry of these defects—at the right-hand side of the interruptions the (2×1) rows show slight protrusions—most certainly reflects an asymmetric STM tip. From the fact that such defects have not been observed in (2×1)O structures formed on clean Cu(110) and from the observation that the density of these defects corresponds reasonably well to the alkali-metal coverage—in this case a density of 0.1 ML is found in the well-ordered areas of the (2×1) reconstruction—we identify these defects with K atoms which have replaced a Cu atom in the added row. This idea of a K-Cu exchange is supported by STM images obtained under different tunneling conditions ($U_T=-0.5$ V, $I_T=6.3$ nA), where the defects are imaged as bright protrusions, which contradicts a simple interpretation as Cu vacancies in the added rows. (Imaging of such vacancies is not expected to depend strongly on tunneling conditions.) The slightly lower concentration of defects compared to the actual alkali-metal coverage may be understood from alkali-metal atom adsorption at antiphase domain boundaries of the (2×1) phase and other structural defects.

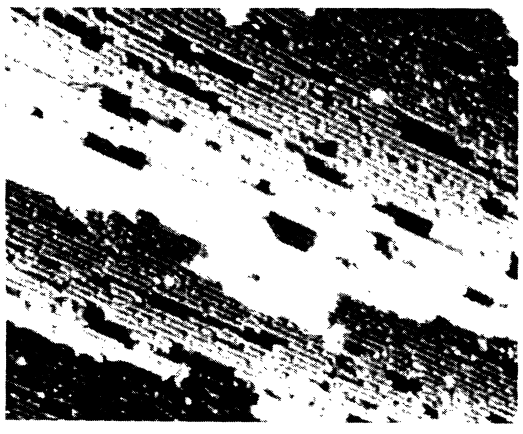

FIG. 3. STM image recorded during oxygen adsorption on K/Cu(110) ($\theta_K=0.13$; 400×330 Å^2; $U_T=-1.6$ V, $I_T=2.5$ nA). Note that due to different imaging conditions the defective [001] added rows in the (2×1)O structure appear as prominent features, differently from Fig. 2. The oxygen dose is 12 L.

A similar sequence of structures was found also for lower K coverages, below the formation of a perfect (1×3) structure. Substituting the potassium by cesium leads to a similar structural scenario as seen for the O/K/Cu(110) system. That is, oxygen adsorption on cesium-precovered Cu(110) surfaces [$\theta_{Cs}=0.13$, which corresponds to the (1×3) reconstruction] leads at first to a pairing of the reconstruction troughs into (1×2) missing-row elements, followed by the formation of compact (1×2) islands, the dissolution of this reconstruction, and the formation of the O/Cu/(110) (2×1) added-row structure.

Upon coadsorption of alkali metals and oxygen on Cu(110) in the lower alkali-metal coverage range strong attractive interactions between the opposite dipoles alkali-metal substrate and oxygen substrate are expected, and even direct chemical bonds between alkali-metal and oxygen atoms might be formed. Indeed, the contraction of the missing-row reconstructed area and the formation of the (1×2) missing-row islands at $\theta_K=0.13$ are indications that some kind of a compound between oxygen and alkali metal exists at low oxygen coverages: In the pure alkali-metal-induced missing-row reconstruction the system attempts to uniformly distribute the missing rows on the surface due to the dipole-dipole repulsion between the alkali-metal atoms. A (1×2) reconstruction in a nonreconstructed surrounding is seen neither for the clean alkali-metal/Cu(110) system nor for O/Cu(110). The fact that the missing rows shrink and cluster in islands upon oxygen adsorption points to an effective attraction between the alkali-metal atoms or the alkali-metal filled troughs, respectively. This can only be rationalized if oxygen is present in these islands. The same conclusion is derived also from the observation that in the beginning

no other oxygen features are seen in STM, although oxygen is clearly detected by AES.

A clear structure identification of the different phases formed during adsorption on the alkali-metal precovered ($\theta_{alk} \leq 0.13$) Cu(110) surfaces is not possible from our STM data. Nevertheless, they provide sufficient structural information for a tentative assignment. As mentioned before, the preferential formation of pairs of missing rows at the beginning of the oxygen exposure [Figs. 2(b) and 2(c)] indicates that these rows are connected by oxygen atoms in between. We speculate that this occurs via local K_2O-type units, which consist of two alkali-metal atoms residing in the missing-row troughs and a connecting oxygen atom localized on the close-packed Cu row between them. A schematic representation of such a K_2O unit is shown in Fig. 4(a). The stability of these structures can be understood from a relatively high binding energy of the oxygen in these K-O-K bridges across the $[1\bar{1}0]$ Cu row due to the negative excess charge density on these Cu atom rows: The alkali-metal–Cu bond is negatively polarized towards the $[1\bar{1}0]$ Cu rows.[18] Hence strong bonds between the electronegative oxygen atoms and these Cu atoms are plausible. Interactions between oxygen and the alkali-metal atoms in the very early stages of oxygen adsorption were observed experimentally for Cs/Ag(110) with $\theta_{Cs}=0.10$.[19] Ag(110) is very similar to Cu(110) with respect to both, its reaction with alkali metal and with oxygen. For Cs/Ag(110) ultraviolet photoemission spectroscopy measurements revealed a downward shift in the energy of the Cs $5p$ states when oxygen was adsorbed on the Cs-precovered surface, which was explained by the presence of negatively polarized oxygen atoms in the direct vicinity. This downward shift occurred at very low oxygen doses and was finished at 1 L, i.e., a strong interaction between the alkali metal and the oxygen exists long before the completion of the (2×1) O/Ag(110) structure, in agreement with our experiments. Similar conclusions can be deduced also from thermal desorption experiments. For O/Cs/Ag(110) ($\theta_{Cs}=0.10$) a second oxygen desorption peak at higher temperatures was attributed to desorption from a more strongly bound state in Cs-O complexes.[19] Such strong, substrate mediated alkali-metal–oxygen bonds have also been proposed for oxygen adsorption on Cs-covered Ru(0001) where a $(\sqrt{3}\times\sqrt{3})R30°$ structure with a Cs-O distance of 3.11 Å was found.[20] In this case also a second, high-temperature desorption peak was found, this time for Cs desorption which is less stable than O_{ad} on that surface.[21]

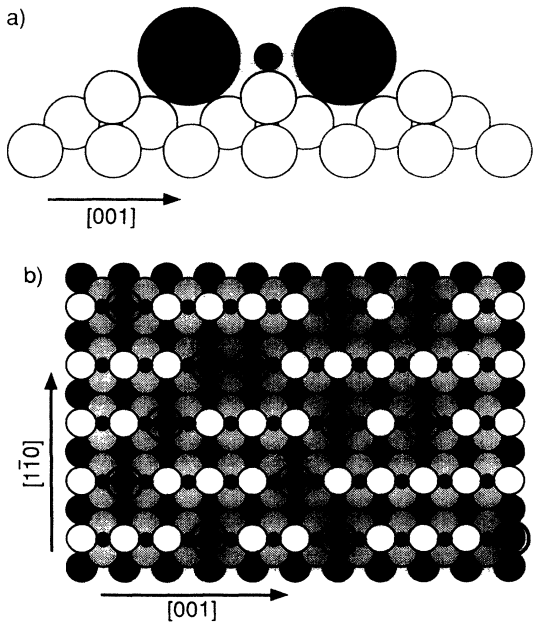

FIG. 4. (a) Schematic model of a K_2O unit in the (1×2) missing-row reconstruction; (b) model of the (2×1)O/alkali/Cu(110) reconstruction (small black circles: oxygen atoms; medium sized circles: Cu atoms; larger, transparent circles: alkali-metal atoms).

In the (2×1) phase the alkali-metal atoms are most likely incorporated in the Cu-O chains. A plausible arrangement of the alkali-metal atoms is shown in Fig. 4(b). We suggest that individual alkali-metal atoms replace individual copper atoms in the Cu-O added-row chains leading to characteristic defects in the (2×1) structure. We did not detect any order in the distribution of these features, indicative of sizeable interactions between them. Hence, in the high oxygen coverage regime the interaction of oxygen with the alkali-metal precovered surface ($\theta_{alk} \leq 0.13$) is structurally dominated by the Cu-O interaction. This is further supported by the observation of the $c(6\times2)$ reconstruction at even higher oxygen coverages, identical to the findings for the pure oxygen/Cu(110) system. The dominance of the Cu-O interaction, at least at oxygen coverages above ~0.2 ML, may be surprising on a first view, because of the strong interactions expected to exist between oxygen and alkali metals. But, it simply reflects the high stability of the Cu-O bond and in particular of the (2×1)O phase. This makes this phase, with not too many defects (≤ 0.13 ML) due to Cu-K exchange in the added rows, more stable than a missing-row alkali-metal phase with a high density of incorporated oxygen adatoms or any other mixed phase with a completely different structure.

B. Oxygen adsorption on the (1×2) reconstructed surface ($\theta_{alk}=0.2$)

Oxygen adsorption on alkali-metal precovered Cu(110) surfaces changes significantly in the coverage range of or above that of the (1×2) reconstruction ($\theta_{alk} \geq 0.2$). First of all, the oxygen coverage does not quasisaturate at about $\theta_O=0.5$, but progresses continuously up to much higher oxygen coverages (Fig. 1). After a dose of 30 L of oxygen the oxygen coverage has increased to $\theta_O=1.1$ for $\theta_{Cs}=0.3$, and even to $\theta_O=1.2$ for $\theta_{Cs}=0.44$. Note that these Cs precoverages are still in the range below a physical monolayer [$\theta_{Cs}=0.48$ (Ref. 14)]. [It should be mentioned that for the higher alkali-metal coverages in Fig. 1 ($\theta_{Cs} \geq 0.3$) the saturation coverage of oxygen is enhanced by about 30% by electron bombardment effects as the AES data are recorded *in situ* during the adsorption. The values found on nonirradiated parts of the surface were $\theta_O=0.75$ for $\theta_{Cs}=0.3$ and $\theta_O=0.95$ for $\theta_{Cs}=0.44$ for a

30-L oxygen exposure.] These data are similar to the numbers reported in the literature: Ernst, Domagala, and Campbell found a saturation O coverage of $\theta_O=1.2$ for an oxygen exposure of 2 L on Cs/Cu(110) with $\theta_{Cs}=0.24$.[22] For $\theta_{Cs}=0.3$ we found the initial sticking coefficient to be close to one, i.e., six times higher than that of the clean surface, in accordance with the findings of Prince and Kordesch for Cs-precovered Ag(110).[19]

The sudden change in the adsorption behavior of oxygen on Cu(110) beyond $\theta_{alk}\approx 0.13$ is different from the trends found on other nonreconstructed alkali-precovered metal surfaces such as Cs/Ru(0001).[21] The STM data shown below suggest that this sudden change is caused by the change in the reconstruction of the Cu(110) surface, which occurs at these coverages.

The structural effects imposed by oxygen adsorption on surfaces with higher alkali-metal precoverages, in this case on the (1×2) reconstructed Cu(110) surface with a K coverage of $\theta_K=0.2$, are shown in Fig. 5. Surprisingly, the initial effects of oxygen are less obvious than for alkali-metal precoverages ≤ 0.13. Until at about 10 L (images are not shown here) the (1×2) reconstruction does not change much, apart from a small number of defects where the alkali metal containing missing-row troughs are interrupted. From the data in Fig. 1 the oxygen coverage after these exposures is estimated to exceed already $\frac{1}{2}$ ML. Only at 14 L [Fig. 5(a)] more apparent changes of the (1×2) reconstruction occur. [Images recorded before that presented in Fig. 5(a), not shown here, reveal that in this case the K-filled troughs of the missing-row reconstruction are imaged as bright lines, which is different from the usual behavior.[16]] In addition to the small defects, where the protruding white lines are interrupted, a number of diagonal elements, connecting neighboring K-filled troughs are resolved. In some areas, e.g., at the right-hand side of the image, the protruding lines representing the former K-filled missing-row troughs exhibit an additional structure along the rows. The lines show a chain structure of small bumps with diameters of approximately 6 Å. This distance comes close to the average spacing of the K atoms in the (1×2) missing-row reconstruction at $\theta_K=0.2$. The structured appearance of these "alkali-metal chains" in the O/K/Cu(110) system is different from the binary K/Cu(110) system where the alkali-metal atoms in the missing-row troughs are mobile at room temperature and had not been resolved in the STM images. It implies that the alkali-metal atoms are pinned by oxygen atoms. The oxygen coverage for the surface shown in Fig. 5(a) is around $\theta_O=0.7$ (directly measured with AES), i.e., the surface area shown in Fig. 5(a) contains, on average, 3 to 4 oxygen atoms per potassium atom. Despite the high oxygen coverage there are no indications for any three-dimensional oxide, i.e., the mixed layer of potassium and oxygen still represents a two-dimensional, adsorbed phase, which displays a clear registry with the underlying substrate. This phase is obviously different from both the oxygen (2×1) reconstruction as well as the (1×2) alkali-metal-induced reconstruction. It cannot be associated with a perturbed reconstruction of one of the binary systems, O/Cu(110) or alkali-metal/Cu(110), in contrast to the situation at $\theta_{alk}\leq 0.13$. We, therefore, assign it to a complex surface compound of potassium and oxygen under participation of Cu.

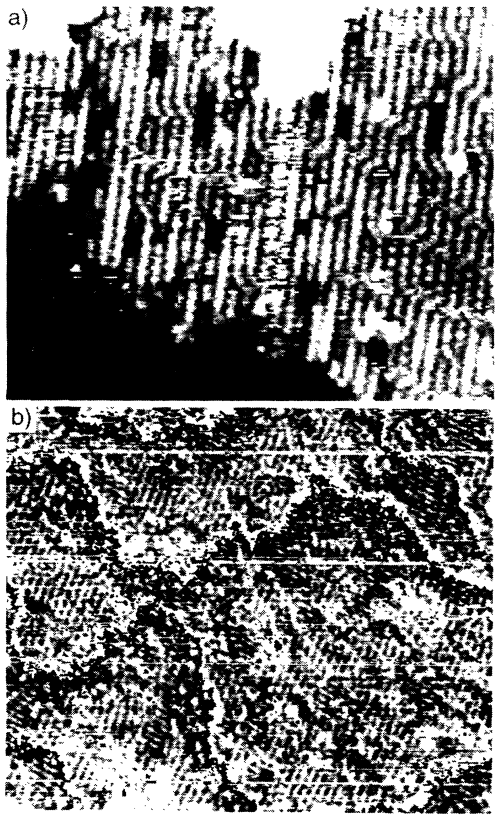

FIG. 5. STM images of oxygen adsorption on the (1×2) reconstructed K/Cu(110) surface at $\theta_K=0.2$; (a) 14 L (240×210 Å^2; $U_T=-0.6$ V, $I_T=6.3$ nA); (b) 44 L (430×360 Å^2; $U_T=-0.5$ V, $I_T=1$ nA).

The lack of long-range mass transport during the formation of this phase indicates that the average density of Cu surface atoms is maintained, i.e., $\theta_{Cu}=0.5$. Hence, this structure equally involves a reconstruction of the Cu(110) substrate. More information, such as the exact adsorption sites of the oxygen, and alkali-metal atoms or the role of the diagonal elements cannot be extracted from the STM images.

With further increasing oxygen exposure the destruction of the row structure continues, and the surface appears more and more disordered, though the terrace structure is still preserved. This is illustrated in Fig. 5(b) after a total oxygen dose of 44 L ($\theta_O=0.75$). For contrast enhancement different terraces are colored with the same gray scale; the terrace edges appear as slightly brighter lines. On these terraces more diagonal elements are found, and small (2×1) patches have evolved. The latter coexist with the "distorted" (1×2) domains on one terrace. The (2×1) structure may be identical to the (2×1) phase formed for $\theta_{alk}\leq 0.13$, i.e., a largely oxygen-induced reconstruction, with alkali-metal atoms dissolved in it. The quality of the STM images in this coverage regime, however, does not allow us to further substantiate

this assignment. The finding of two different phases in this alkali-metal coverage regime agrees well with the metastable deexcitation spectroscopy results of Woratschek *et al.*,[23] where two sets of oxygen-induced spectral features were seen after oxygen exposure on the Cs saturated surface. A similar observation of two phases was reported by Kiskinova, Rangelov, and Surnev for O/K,Cs/Ru(0001),[21] who found patches with different work functions on the surface for $\theta_{Cs} > 0.14$ and $\theta_O > 0.5$.

Hence, for alkali-metal precoverages higher than those necessary to complete the (1×2) reconstruction, i.e., $\theta_{alk} \geq 0.2$, the adsorption behavior and the surface structures induced by oxygen adsorption are drastically altered. Under these conditions the effect of the alkali metal is no longer limited to an increase of the sticking coefficient or to a perturbation of the (2×1) O/Cu(110) structure by inclusion of small alkali-metal defects.

IV. CONCLUSIONS

We have shown that the oxidation of submonolayers of alkali metals on the Cu(110) surface proceeds via various (ordered) phases, all of which involve a reconstruction of the Cu(110) substrate. The actual structures depend on the respective alkali-metal and oxygen coverages. These results and the absence of three-dimensional alkali-metal oxides indicate that the energetics of the adsorption system are largely determined by adsorbate-substrate bonds. Interactions between the adsorbates do, however, affect the reconstruction itself: After oxygen adsorption for low alkali-metal coverages, they lead to an instantaneous contraction of the missing rows into local (1×2) islands, which we suggest are stabilized by $(\text{alkali-metal})_2O$ units bridging the $[1\bar{1}0]$Cu rows. This missing-row alkali-metal–oxygen structure is unstable and undergoes a transition into a defective (2×1) added-row structure with continuing oxygen exposure. This latter phase does not constitute a compound of alkali metal and oxygen, but rather resembles the (2×1) O/Cu(110) reconstruction, with the alkali-metal atoms statistically dissolved in the added rows.

For oxygen adsorption on the (1×2) missing-row structure, i.e., for $\theta_{alk}=0.2$, a new reconstructed phase is formed. It is characterized by immobilized alkali-metal atoms and diagonal elements between neighboring (1×2) troughs. We ascribe this structure to a complex surface compound of the alkali metal and oxygen. Further oxygen exposure leads to a phase separation into complex (1×2), (2×1), and diagonal O–alkali-metal–Cu structures. In addition to the O–alkali-metal–Cu structures also the oxygen saturation coverage depends strongly on the alkali-metal precoverage: Whereas at alkali-metal coverages up to $\theta_{alk} \leq 0.13$ the oxygen coverage does not exceed $\theta_O=0.5$ [the $c(6\times2)$ structure is found only at much higher oxygen exposures], alkali-metal precoverages above $\theta_{alk}=0.2$ lead to oxygen coverages well above $\theta_O=0.5$ which are accommodated in complex intermixed structures.

*Permanent address: Abteilung Oberflächenchemie und Katalyse, Universität Ulm, D-89069 Ulm, Germany.

[1]Z. Paál, G. Ertl, and S. B. Lee, Appl. Surf. Sci. **8**, 231 (1981).
[2]R. J. Behm, D. K. Flynn, K. D. Jamison, G. Ertl, and P. A. Thiel, Phys. Rev. B **36**, 9267 (1987).
[3]W. C. Fan and A. Ignatiev, Phys. Rev. B **38**, 366 (1988).
[4]W. C. Fan and A. Ignatiev, J. Vac. Sci. Technol. A **6**, 735 (1988).
[5]R. Schuster, J. V. Barth, G. Ertl, and R. J. Behm, Surf. Sci. Lett. **247**, L229 (1991).
[6]R. Schuster, J. V. Barth, G. Ertl, and R. J. Behm, Phys. Rev. B **44**, 13 689 (1991).
[7]R. Schuster, J. V. Barth, R. J. Behm, and G. Ertl, Phys. Rev. Lett. **69**, 2547 (1992).
[8]R. J. Behm, in *Physics and Chemistry of Alkali Metal Adsorption,* edited by H. P. Bonzel, A. M. Bradshaw, and G. Ertl (Elsevier, Amsterdam, 1989), Vol. 57, p. 111; R. Schuster, J. V. Barth, G. Ertl, and R. J. Behm, Phys. Rev. B **44**, 13 689 (1991), and references therein.
[9]D. J. Coulman, J. Wintterlin, R. J. Behm, and G. Ertl, Phys. Rev. Lett. **64**, 1761 (1990).
[10]F. Jensen, F. Besenbacher, E. Laegsgaard, and I. Stensgaard, Phys. Rev. B **41**, 10 233 (1990).
[11]Y. Kuk, F. M. Chua, P. J. Silverman, and J. A. Meyer, Phys. Rev. B **41**, 12 393 (1990).
[12]R. Feidenhans'l, F. Grey, M. Nielsen, F. Besenbacher, F. Jensen, E. Laegsgaard, I. Stensgaard, K. W. Jacobsen, J. N. Nørskov, and R. L. Johnson, Phys. Rev. Lett. **65**, 2027 (1990).
[13]D. Coulman, J. Wintterlin, J. V. Barth, and G. Ertl, Surf. Sci. **240**, 151 (1990).
[14]W. D. Clendening, J. A. Rodriguez, J. M. Campbell, and C. T. Campbell, Surf. Sci. **216**, 429 (1989).
[15]J. V. Barth, R. Schuster, J. Wintterlin, G. Ertl, and R. J. Behm (unpublished).
[16]G. Doyen, D. Drakova, J. V. Barth, R. Schuster, T. Gritsch, R. J. Behm, and G. Ertl, Phys. Rev. B **48**, 1738 (1993).
[17]J. Wintterlin, R. Schuster, D. J. Coulman, and G. Ertl, J. Vac. Sci. Technol. B **9**, 902 (1991).
[18]K. W. Jacobsen and J. K. Nørskov, Phys. Rev. Lett. **60**, 2496 (1988).
[19]K. C. Prince and M. E. Kordesch, Appl. Surf. Sci. **22/23**, 469 (1985).
[20]H. Over, H. Bludau, M. Skottke-Klein, W. Moritz, and G. Ertl, Phys. Rev. B **46**, 4360 (1992).
[21]M. Kiskinova, G. Rangelov, and L. Surnev, Surf. Sci. **172**, 57 (1986).
[22]K. H. Ernst, M. E. Domagala, and C. T. Campbell, Surf. Sci. **259**, 18 (1991).
[23]B. Woratschek, W. Sesselmann, J. Küppers, G. Ertl, and H. Haberland, J. Chem. Phys. **86**, 2411 (1987).

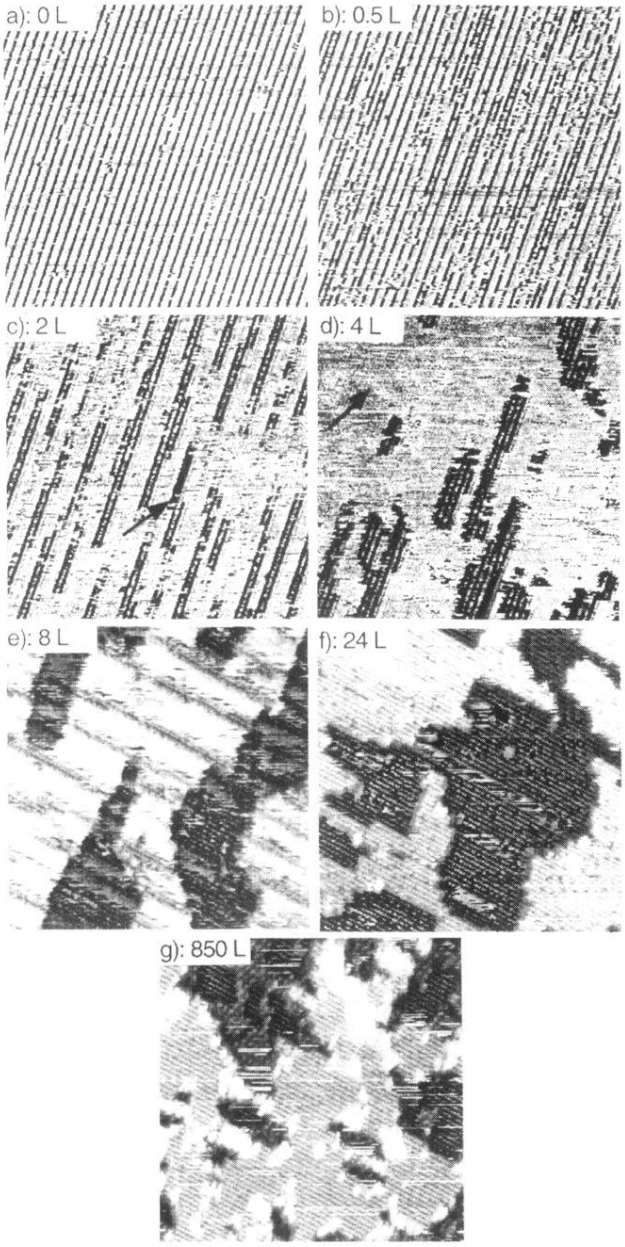

FIG. 2. STM images recorded during oxygen adsorption on the potassium-precovered Cu(110) surface, with $\theta_K = 0.13$ (360×360 Å^2; $U_T = -0.03$ V, $I_T = 6.3$ nA). The oxygen doses are indicated. In Fig. 2(c) the dissolution of $[1\bar{1}0]$Cu rows in the (1×2) structure and in Fig. 2(d) the nucleation of the (2×1)O structure are marked with arrows.

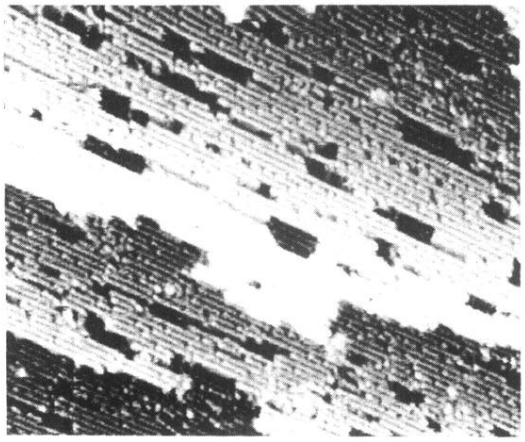

FIG. 3. STM image recorded during oxygen adsorption on K/Cu(110) ($\theta_K = 0.13$; 400×330 Å^2; $U_T = -1.6$ V, $I_T = 2.5$ nA). Note that due to different imaging conditions the defective [001] added rows in the (2×1)O structure appear as prominent features, differently from Fig. 2. The oxygen dose is 12 L.

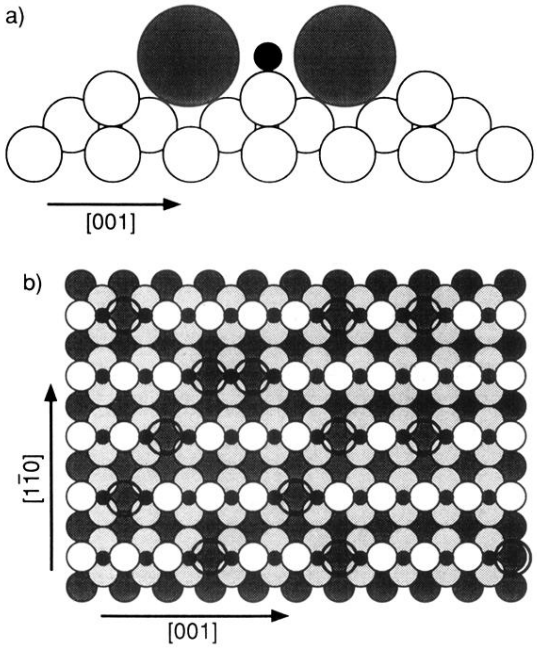

FIG. 4. (a) Schematic model of a K_2O unit in the (1×2) missing-row reconstruction; (b) model of the (2×1)O/alkali/Cu(110) reconstruction (small black circles: oxygen atoms; medium sized circles: Cu atoms; larger, transparent circles: alkali-metal atoms).

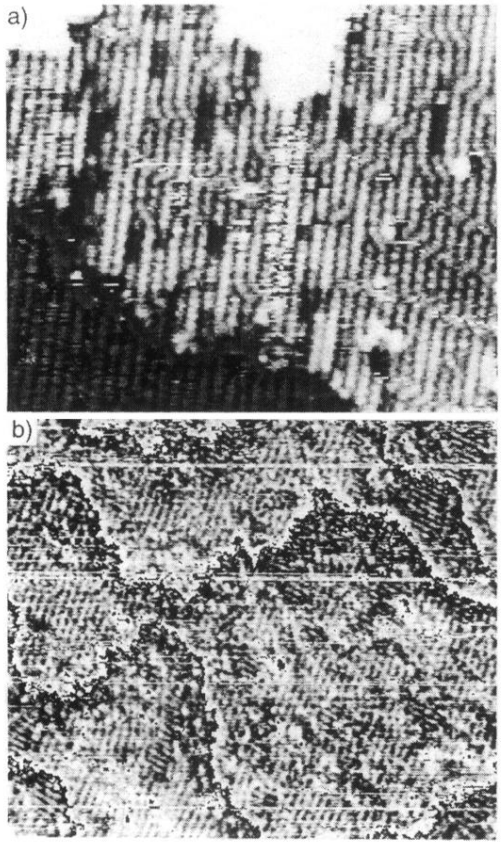

FIG. 5. STM images of oxygen adsorption on the (1×2) reconstructed K/Cu(110) surface at $\theta_K = 0.2$; (a) 14 L (240×210 Å^2; $U_T = -0.6$ V, $I_T = 6.3$ nA); (b) 44 L (430×360 Å^2; $U_T = -0.5$ V, $I_T = 1$ nA).